Regulation of gene expression and signaling pathway activity in mammalian cells by automated microfluidics feedback control.

Lorena Postiglione[1], Sara Napolitano[1]*, Elisa Pedone[2,3,]*, Daniel L. Rocca[2,3,4,]*, Francesco Aulicino[4,5], Marco Santorelli[1], Barbara Tumaini[1], Lucia Marucci[2,3,4]#, Diego di Bernardo[1,6]#

[1] Telethon Institute of Genetics and Medicine, Via Campi Flegrei 34 80078 Pozzuoli (NA), Italy

[2]Department of Engineering Mathematics, University of Bristol, Bristol BS8 1UB, UK

[3]School of Cellular and Molecular Medicine, University of Bristol, Bristol BS8 1UB, UK

[4]BrisSynBio, Bristol BS8 1TQ, UK

[5]Department of Biochemistry, University of Bristol, Bristol BS8 1UB, UK

[6]Department of Chemical, Materials and Industrial Engineering, University of Naples Federico II, Piazzale V. Tecchio 80, 80125 Naples, Italy

*These authors contribute equally to this work.

#co-corresponding; dibernardo@tigem.it; lucia.marucci@bristol.ac.uk

Keywords: Control Engineering, Microfluidics, Synthetic Biology

Abstract

Gene networks and signalling pathways display complex topologies and, as a result, complex non-linear behaviours. Accumulating evidence shows that both static (concentration) and dynamical (rate-of-change) features of transcription factors, ligands and environmental stimuli control downstream processes and ultimately cellular functions. Currently, however, methods to generate stimuli with desired features to probe cell response are still lacking. Here, combining tools from Control Engineering and Synthetic Biology (Cybergenetics), we propose a simple and cost-effective microfluidics-based platform to precisely regulate gene expression and signalling pathway activity in mammalian cells by means of real-time feedback control. We show that this platform allows: (i) to automatically regulate gene expression from inducible promoters in different cell types, including mouse embryonic stem cells; (ii) to precisely regulate the activity of the mTOR signalling pathway in single cells; (iii) to build a bio-hybrid oscillator in single embryonic stem cells by interfacing biological parts with virtual *in silico* counterparts. Ultimately, this platform can be used to probe gene networks and signalling pathways to understand how they process static and dynamic features of specific stimuli, as well as for the rapid prototyping of synthetic circuits for biotechnology and biomedical purposes.

Mammalian cells are dynamical systems. They detect, adapt and respond to time-varying inputs such as environmental cues, secreted molecules, and mechanical stimuli. These processes are controlled by genes, proteins, small molecules, and their mutual interactions giving rise to gene networks and signalling pathways, often including positive and negative feedback loops. Such gene networks can exhibit nonlinear behaviours, such as multistability and oscillatory dynamics, with important consequences for cellular phenotypes. Despite their individual components being well characterised, *operational* understanding of how these regulatory networks work is still lacking[1]. Indeed, understanding how they process and respond to time-varying stimuli and ultimately modify cell behaviour will enable rational modification of cellular processes, an essential capability for biomedicine and biotechnology. Currently, however, it is very difficult, if not impossible in some cases, to apply stimuli with desired amplitudes and temporal dynamics, rather coarse stimuli are often used (i.e. gene over-expression, knock-down, adding or removing a ligand), thus preventing full exploration of network behaviour[2,3]. The nascent field of Cybergenetics explores how Control Engineering principles can be applied to dynamically steer biological processes at will[4,5]. Successful attempts to design control systems to dynamically regulate gene expression have been recently reported in the literature[6], but mainly in prokaryotes and single-cell eukaryotes[7–13]. Control systems usually employ a negative feedback approach, where a control algorithm decides the amplitude and duration of the stimulus (e.g. small molecule, ligand, light) to apply to the cell to minimize the difference between the measured and the target fluorescence levels. Experimental control platforms have been implemented using both microfluidics and optogenetics approaches, with the latter reducing actuation time, but requiring significant genetic modification to cells in order to make them responsive to the light input. The application of control engineering to mammalian systems is still very limited.[14] The reason for the slower progress can be attributed to different factors: increased experimental time and costs required to genetically engineer a mammalian cell, slower overall dynamics, and increased sensitivity to environmental conditions (e.g. phototoxicity, shear stress, etc.). All together these factors make the application of control engineering to mammlian cells much more challenging. We recently described a microfluidics platform enabling automatic regulation of gene expression from drug-inducible promoters in mammalian cells[15]. The experimental set-up (Figure 1a) consists of a microfluidic device hosted in an inverted fluorescence microscope and two syringes whose position is automatically controlled by stepper motors and connected to the device cell chambers in order to dynamically change the concentration of an inducer molecule[10,11,15 16]. Here, by means of a microfluidics-based platform, we make it possible to precisely and robustly control both gene expression and signalling pathway activity in mammalian cells of biotechnological and biomedical interest, including stem cells (Figure 1b). We also implement a bio-hybrid circuit combining biological parts with "virtual" *in-*

silico parts in stem cells to speed up prototyping of biomolecular circuits for Synthetic Biology applications, with relevance to regenerative medicine[17].

Results

Overview of the control platform. A schematic representation of the experimental platform is shown in Figure 2a. A computer controls the whole platform by: (i) acquiring images at predefined time intervals; (ii) performing image analysis to quantify the phenotype of interest in cells, by means of fluorescent reporters, and the level of the inducer molecule in the device cell chambers, by means of a fluorescent dye; (iii) executing the *biological system controller* to compute the necessary amount and duration of inducer molecule treatment (*control input*) for the fluorescence to reach its target value (*reference*); (iv) executing the *inducer molecule controller* to move two motor-controlled syringes to provide inducer molecule to the cells according to the *control input* (Supporting Information).

Both the inducer molecule controller and the biological system controller follow the Model Predictive Control strategy (MPC), which has previously been applied to control biological systems but never in mammalian cells[8,9,11,12] (Supporting Information). The MPC strategy is preferred to simpler input-output controllers (e.g. PID) as it naturally allows to include experimental constrains such as sampling time and bounded control input in the controller design.

Two motor-controlled syringes, shown in Figure 2b, provide a (time-varying) concentration of an inducer molecule by mixing two fluids (medium with inducer plus fluorescent dye or standard medium). Figure 2c shows an example of an inducer molecule tracking control experiments (Supporting Information, Figure S6) where the concentration of tetracycline in the microfluidics cell chamber was automatically regulated by the inducer molecule controller to track a target time-varying concentration (staircase and ramp).

Control of gene expression in Chinese Hamster Ovary cells. We assessed the feasibility of precisely regulating the expression of a gene of interest from an inducible promoter by means of automated microfluidics feedback control. We stably integrated in Chinese Hamster Ovary (CHO) cells (Figure 1b) a tetracycline responsive promoter[18] driving the expression of a fluorescent reporter protein ($Ub^{V76}GFP$) destabilised both at the mRNA and protein level[19]. These cells constitutively express the artificial tetracycline-responsive transcriptional activator tTA. When tetracycline is administered to the cells, tTA is not able to bind the promoter preventing expression of the fluorescent report (TET-OFF system). We used a destabilised mRNA, in addition to a destabilised protein, to maximally speed up system dynamics, as these are dictated by both mRNA and protein degradation rates.[19] Indeed, in the absence of the mRNA degradation tag, the dynamics of the system are dominated by the $Ub^{V76}GFP$ mRNA, whose half-life is about 130 min[19], even

though the $Ub^{V76}GFP$ protein half-life is just 20 min[19]. On the contrary, when the 3'UTR degradation tag was added, the mRNA half-life became 18 min[19], thus considerably speeding up the system. In our previous proof-of-principle study[15], we used a slower degrading protein with an half life of 2 hours (d2YFP) with no mRNA destabilisation. The resulting system dynamics were much slower (Figure 3b in Fracassi et al[15]) causing the system to exhibit oscillation when using a PI controller. Moreover, in Supplementary Figure 3 in Fracassi et al[15], we simulated the action of an MPC controller on that system and found that whereas oscillations disappered, the time taken to reach the set-point was predicted to be approximately 13 hours, thus prompting us to speed up the system dynamics in this current study. We carried out a series of set-point control experiments (Figure 3) to bring the expression of the fluorescent reporter in the cell population at 50% of its maximal value (i.e. stationary expression when no tetracycline is provided to the cells). Achieving and maintaining such level using a classical approach would be very difficult, as tetracycline concentration would have to be precisely titrated due to the strong nonlinearity of the inducible promoter. One syringe is filled with standard growth medium and the other with standard growth medium supplemented with tetracycline at a concentration of 100ng/ml plus sulforhodamine to track tetracycline concentration. We applied two different MPC strategies (Supporting Information) to a set-point control task, one considering a bang-bang control input (i.e. providing either no tetracycline or the maximum concentration of tetracycline), the other considering a continuous control input (i.e. the controller chooses any tetracycline concentration between 0 and 100ng/ml, Supporting Information). The dynamical models used for the implementation of the two MPC strategies are reported in Figures S1 and S2. The results of control experiments are shown in Figure 3, Figure S3 and Movies S1-S4. Cells reached and maintained the desired fluorescence value across the cell population without exhibiting oscillations, vastly improving our previous results obtained with Relay and Proportional-Integral controllers[15]. Interestingly, and as expected from optimal control theory, even in the case of continuous control inputs, the MPC algorithm chose as the best strategy to achieve the target expression level a bang-bang control input before converging to a fixed concentration of about 50ng/ml (Figure 3c,d). It is likely that the actual tetracycline concentration in the cell chamber in the case of a bang-bang control input (Figure 3a,b) is indeed a filtered version of the control input because of the delay in the action of the actuator (syrenges and diffusion of the medium), effectively making the two strategies (bang-bang and continuos) similar at the level of actual tetracycline concentration in the cell chamber, which may explain why the performances are so comparable.

Control of gene expression in mouse Embryonic Stem Cells. To test the generality of our approach, we applied automated microfluidics feedback control to regulate gene expression in a more complex cell type by means of an alternative inducible system. We engineered mouse

Embryonic Stem Cells (mESCs) to express the TET-ON transcriptional transactivator tTA and a Degradation Domain (DD) fused mCherry protein from a doxycycline-inducible promoter (Figure 1b and Supporting Information). In these cells, reporter expression from the inducible promoter is only possible in the presence of the tetracycline analog doxycycline (Dox); furthermore, the small-molecule ligand trimethoprim (TMP) destabilises the protein in a reversible and dose-dependent manner, allowing for post-translational control[20,21]. In the set-point control experiments (Figure 4 and Movies S5,S6), we successfully applied the MPC strategy with a bang-bang control input to regulate the expression of the reporter protein at 50% of its maximal value (Supporting Information). The dynamical model used for the implementation of the MPC strategy is reported in Figure S4.

Single-cell control of mTOR signalling pathway activity. We then applied automated microfluidics feedback control to steer the activity of the mTOR pathway in a single cell. It has been recently demonstrated that the mTOR pathway controls the activity of the transcription factor EB (TFEB), a key player in transcriptional regulation of lysosomal biogenesis and autophagy[22,23]. This control is mediated by mTORC1 phosphorylation of TFEB, the latter being sequestered in the cytoplasm. During amino-acid starvation, mTOR signaling is negatively regulated, hence TFEB is no longer phosphorylated and it accumulates in the nucleus inducing transcription of its target genes[24]. The nuclear accumulation of TFEB can thus be used as a quantitative biomarker of mTOR signalling activity[22,25]. We generated HeLa cells stably expressing a TFEB-GFP fusion protein from a constitutive promoter, in addition to a nuclear mCherry protein to facilitate image analysis (Figure 1b and Supporting Information). The variable to be controlled is the nuclear TFEB-GFP fluorescence, acting as a quantitative proxy of mTOR activity, whereas the control input is the mTOR inhibitor Torin-1[26] (Figure S5 and Supporting Information). We applied an MPC strategy (Supporting Information) considering a bang-bang control input (i.e. providing either no Torin-1 or the maximum concentration of Torin-1). All of the experiments start with a calibration phase of 180 min in the presence of Torin-1 to estimate the maximal TFEB-GFP nuclear fluorescence when mTOR signalling is inhibited. We performed single-cell set-point control experiments, to bring TFEB-GFP nuclear fluorescence to 50% of its maximum value (Figure 5a,b and Movies S7,S8), as well as single-cell signal tracking experiments, where TFEB-GFP nuclear fluorescence must follow a time-varying reference (Figure 5c,d and Movies S9,S10).

Biohybrid oscillator in mouse embryonic stem cells. Hybrid genetic circuits built by interfacing biological systems with virtual *in silico* counterparts have been recently demonstrated in bacteria[17]. These Bio-Hybrid circuits can be used to quickly test hypotheses on the regulatory logic of gene networks and to prototype synthetic circuits. Here, we built a hybrid genetic oscillator in mESC expressing a DDmCherry protein from the doxycycline inducible promoter (Figure 1b). The hybrid

oscillator, shown in Figure 6a, is based on a delayed negative feedback loop mechanism, where cyclic gene expression is mediated by direct, or indirect, repression of the gene promoter by its protein product, after a delay that enables protein accumulation[27]. We 'virtualised' the transcriptional repression signal so that DDmCherry can inhibit its own expression. This is accomplished by implementing a 'virtual promoter' *in silico* by means of the microfluidics platform (Figure 6b and Movie S11). At regular sampling times (60 min), mCherry fluorescence in the cell population is compared to a threshold level. If fluorescence is below the threshold, the promoter is activated by providing Dox+TMP to the cells, otherwise standard medium is provided. We chose the threshold to be 50% of the maximum fluorescence when cells are grown in the presence of Dox+TMP (Supporting Information). As microscopic images are taken at 60 min intervals, there is a minimum 60 min delay between the measurement of mCherry fluorescence and the delivery of the input to the cells. However, the effective delay (τ in Figure 6a) could be greater as this is affected also by DDmCherry transcription, translation and protein stability. We reasoned that the hybrid circuit should be able to generate oscillations because it would act as a delayed negative feedback loop. As shown in Figure 6c, periodic oscillations in fluorescence were indeed observed with a period of 490 min. In order to estimate the effective delay from the data, we used a simple mathematical model of a delayed negative feedback oscillator (Supporting Information). By fitting the model parameters to the data in Figure 6c, we obtained an estimate of the effective delay of 107 min, which, as expected, is greater than the 60 min sampling delay.

Discussion

In this work, we proved the generality and usefulness of the automated microfluidics feedback control platform for different applications and experimental testbeds. This technology can be easily implemented in any lab without specific training and at very limited costs, as it is based on the Dial-a-Wave system[28], which does not require any dedicated pumps or valve and for which online tutorial guides are available (http://biodynamics.ucsd.edu/).

We have previously described a proof-of-concept approach to control gene expression in a microfluidics/microscopy set-up in a mammalian cell line[15]. Our initial work, however, was limited to set-point regulation of gene expression in single cell-line (CHO) using a rudimentary controller (Relay) which was unable to cope with oscillations around the set-point. Here, by means of a redesigned microfluidics-based platform, we precisely and robustly control both gene expression and endogenous signalling pathway activity in different mammalian cells of biotechnological and biomedical interest, including stem cells for the first time, with single-cell precision. We introduced a model-based control algorithm, which allowed us to cope with the slow response to inducer

molecules preventing oscillations to occur, and an inducer molecule controller, which enable precise regulation of its concentration in time.

We demonstrated that it is possible to precisely regulate gene expression in CHO cells and mouse embryonic stems cells (mESCs) from inducible promoters. CHO cells are of extreme biotechnological interest and the workhorse in industry for recombinant protein production[29]. Optimisation of the production process, however, requires the ability to accurately control the level and timing of gene expression in the host cell factory during the manufacturing process[30]. The automated microfluidics feedback control platform is an enabling technology in this setting and could be used for identifying optimal conditions for protein production in continuously perfused production processes, or to regulate the level of a protein product that is toxic if highly expressed.

Our results also pioneer the application of microfluidics-based control of gene expression in mESCs and pave the way for more sophisticated control of cellular behaviour in the context of regenerative medicine. Indeed, the dynamic expression of pluripotency genes is essential for cell fate determination[31–36], hence being able to control their dynamics at will provides researchers with unprecedented opportunities.

We also showed that it is possible to dynamically regulate in individual cells the activity of the mammalian target of rapamycin (mTOR), a key regulator of cell growth, metabolism and proliferation[37,38] whose dysregulation often underlies common diseases such as cancer[39]. Precise control of the mTOR signalling pathway activity will make it possible to quantitatively and dynamically study how mTOR regulates downstream biological processes such as autophagy, a key pathway of extreme interest for the therapy of neurodegenerative disorders.

Finally, we showed that our platform can be used to synthetise a hybrid genetic oscillator by interfacing biomolecular circuits with virtual *in silico* components. In the context of synthetic biology, bio-hybrid circuits may allow rapid prototyping of synthetic circuits, thus speeding up the development phase and hence broadening applicability.

Our approach is generasible to control other celluler features in addition to gene expression and protein localisation, such as cellular morphology. Indeed, any feature can be used as 'output' of the biological system to be controlled, as long as there is a molecule or treatment that can be used as 'input' to modify the chosen output.

Associated Content

Supporting Information

Model Identification, control strategies implementation, microscopy and image analysis, cellular constructs, microfluidic platform. Movies showing the control experiments.

Acknowledgements

This work was supported in part by the COSY-BIO project, that has received funding from the European Union's Horizon 2020 under grant agreement No 766840 to DdB and LM, by Fondazione Telethon grant to DdB, by the Medical Research Council grant MR/N021444/1 to LM, by the Engineering and Physical Sciences Research Council grant EP/R041695/1 to LM, and by BrisSynBio, a BBSRC/EPSRC Synthetic Biology Research Centre (BB/L01386X/1) to LM. LP was supported by a University of Naples "Federico II" doctoral fellowship.

Author Contributions

LP implemented the control strategy and analysed the data. LP designed and performed the experiments in CHO cells. LP and SN designed and performed the experiments in HeLa cells. LP, EP and DR designed and performed the experiments in stem cells. FA, MA and BT performed molecular cloning and generated monoclonal populations. LM and DDB conceived ideas. LP and DDB wrote the manuscript with input from EP, DR and LM. DDB supervised the research.

References

1. Antebi, Y. E., Nandagopal, N. & Elowitz, M. B. An operational view of intercellular signaling pathways. *Curr. Opin. Syst. Biol.* **1,** 16–24 (2017).

2. Babtie, A. C., Kirk, P. & Stumpf, M. P. H. Topological sensitivity analysis for systems biology. *Proc. Natl. Acad. Sci. U. S. A.* **111,** 18507–12 (2014).

3. Banga, J. R. Optimization in computational systems biology. *BMC Syst. Biol.* **2,** 47 (2008).

4. Briat, C. & Khammash, M. Perfect Adaptation and Optimal Equilibrium Productivity in a Simple Microbial Biofuel Metabolic Pathway Using Dynamic Integral Control. doi:10.1021/acssynbio.7b00188

5. Lugagne, J.-B. *et al.* Balancing a genetic toggle switch by real-time feedback control and periodic forcing. *Nat. Commun.* **8,** 1671 (2017).

6. Del Vecchio, D., Dy, A. J. & Qian, Y. Control theory meets synthetic biology. *J. R. Soc. Interface* **13,** 20160380 (2016).

7. Danino, T., Mondragón-Palomino, O., Tsimring, L. & Hasty, J. A synchronized quorum of genetic clocks. *Nature* **463,** 326–330 (2010).

8. Milias-Argeitis, A. *et al.* In silico feedback for in vivo regulation of a gene expression circuit.

Nat. Biotechnol. **29,** 1114–1116 (2011).

9. Uhlendorf, J. *et al.* Long-term model predictive control of gene expression at the population and single-cell levels. *Proc. Natl. Acad. Sci. U. S. A.* **109,** 14271–6 (2012).

10. Menolascina, F. *et al.* In-Vivo Real-Time Control of Protein Expression from Endogenous and Synthetic Gene Networks. *PLoS Comput. Biol.* **10,** (2014).

11. Fiore, G., Perrino, G., di Bernardo, M. & di Bernardo, D. *In Vivo* Real-Time Control of Gene Expression: A Comparative Analysis of Feedback Control Strategies in Yeast. *ACS Synth. Biol.* **5,** 154–162 (2016).

12. Milias-Argeitis, A., Rullan, M., Aoki, S. K., Buchmann, P. & Khammash, M. Automated optogenetic feedback control for precise and robust regulation of gene expression and cell growth. *Nat. Commun.* **7,** 12546 (2016).

13. Olson, E. J., Hartsough, L. A., Landry, B. P., Shroff, R. & Tabor, J. J. Characterizing bacterial gene circuit dynamics with optically programmed gene expression signals. *Nat. Methods* **11,** 449–455 (2014).

14. Toettcher, J. E., Gong, D., Lim, W. A. & Weiner, O. D. Light-based feedback for controlling intracellular signaling dynamics. *Nat. Methods* **8,** 837–839 (2011).

15. Fracassi, C., Postiglione, L., Fiore, G. & Di Bernardo, D. Automatic Control of Gene Expression in Mammalian Cells. *ACS Synth. Biol.* **5,** 296–302 (2016).

16. Kolnik, M., Tsimring, L. S. & Hasty, J. Vacuum-assisted cell loading enables shear-free mammalian microfluidic culture. *Lab Chip* **12,** 4732 (2012).

17. Chait, R., Ruess, J., Bergmiller, T., Tkačik, G. & Guet, C. C. Shaping bacterial population behavior through computer-interfaced control of individual cells. doi:10.1038/s41467-017-01683-1

18. Gossen, M. & Bujard, H. Tight control of gene expression in mammalian cells by tetracycline-responsive promoters. *Proc. Natl. Acad. Sci. U. S. A.* **89,** 5547–51 (1992).

19. Santorelli, M. *et al.* Reconstitution of an Ultradian Oscillator in Mammalian Cells by a Synthetic Biology Approach. *ACS Synth. Biol.* **7,** 1447–1455 (2018).

20. Iwamoto, M., Björklund, T., Lundberg, C., Kirik, D. & Wandless, T. J. A General Chemical Method to Regulate Protein Stability in the Mammalian Central Nervous System. *Chem. Biol.* **17,** 981–988 (2010).

21. Sui, D. *et al.* Stem Cell Reports Fine-Tuning of iPSC Derivation by an Inducible

Reprogramming System at the Protein Level. (2014). doi:10.1016/j.stemcr.2014.03.013

22. Settembre, C. *et al.* A lysosome-to-nucleus signalling mechanism senses and regulates the lysosome via mTOR and TFEB. *EMBO J.* **31,** 1095 LP-1108 (2012).

23. Sardiello, M. *et al.* A gene network regulating lysosomal biogenesis and function. *Science* **325,** 473–7 (2009).

24. Settembre, C., Fraldi, A., Medina, D. L. & Ballabio, A. Signals from the lysosome: A control centre for cellular clearance and energy metabolism. *Nat. Rev. Mol. Cell Biol.* **14,** 283–296 (2013).

25. Medina, D. L. *et al.* Lysosomal calcium signalling regulates autophagy through calcineurin and TFEB. *Nat. Cell Biol.* **17,** 288–99 (2015).

26. Thoreen, C. C. *et al.* An ATP-competitive mammalian target of rapamycin inhibitor reveals rapamycin-resistant functions of mTORC1. *J. Biol. Chem.* **284,** 8023–32 (2009).

27. Novák, B. & Tyson, J. J. Design principles of biochemical oscillators. *Nat. Rev. Mol. Cell Biol.* **9,** 981–991 (2008).

28. Ferry, M. S., Razinkov, I. A. & Hasty, J. Microfluidics for Synthetic Biology: From Design to Execution. *Synth. Biol. Part A* **497,** 295–372 (2011).

29. Wurm, F. M. Production of recombinant protein therapeutics in cultivated mammalian cells. *Nat. Biotechnol.* **22,** 1393–1398 (2004).

30. Brown, A. J. & James, D. C. Precision control of recombinant gene transcription for CHO cell synthetic biology. *Biotechnol. Adv.* **34,** 492–503 (2016).

31. Torres-Padilla, M.-E. & Chambers, I. Transcription factor heterogeneity in pluripotent stem cells: a stochastic advantage. *Development* **141,** 2173–81 (2014).

32. Abranches, E. *et al.* Stochastic NANOG fluctuations allow mouse embryonic stem cells to explore pluripotency. *Development* **141,** 2770–9 (2014).

33. Kalmar, T. *et al.* Regulated Fluctuations in Nanog Expression Mediate Cell Fate Decisions in Embryonic Stem Cells. *PLoS Biol.* **7,** e1000149 (2009).

34. Marucci, L. *et al.* β-Catenin Fluctuates in Mouse ESCs and Is Essential for Nanog-Mediated Reprogramming of Somatic Cells to Pluripotency. *Cell Rep.* **8,** 1686–1696 (2014).

35. Godwin, S. *et al.* An extended model for culture-dependent heterogenous gene expression and proliferation dynamics in mouse embryonic stem cells. *npj Syst. Biol. Appl.* **3,** 19 (2017).

36. Marucci, L. Nanog Dynamics in Mouse Embryonic Stem Cells: Results from Systems Biology Approaches. *Stem Cells Int.* **2017,** 1–14 (2017).

37. Mizushima, N. & Komatsu, M. Autophagy: Renovation of cells and tissues. *Cell* **147,** 728–741 (2011).

38. Sabatini, D. M., Cantley, L. C. & Goldstein, J. L. Twenty-five years of mTOR: Uncovering the link from nutrients to growth. doi:10.1073/pnas.1716173114

39. Di Malta, C. *et al.* Transcriptional activation of RagD GTPase controls mTORC1 and promotes cancer growth. *Science (80-.).* **356,** 1188–1192 (2017).

Figures:

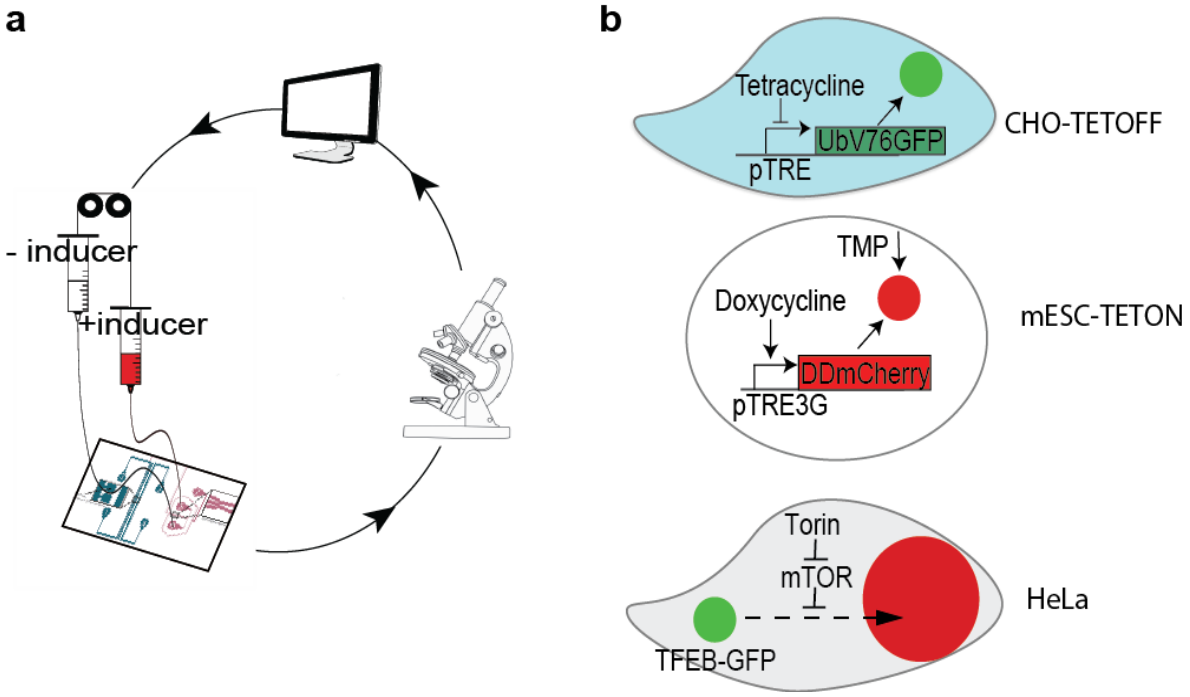

Figure 1. Automated microfluidics feedback control platform and cellular models. **(a)** The platform consists of a microfluidic device, a time lapse microscopy and a set of automated syringes, all controlled by a computer. Cells grow in a microfluidic device within a temperature- and CO2-controlled environment under an inverted fluorescence microscope. Images are acquired at regular sampling time, and quantification of the fluorescence is performed via an image segmentation algorithm. A control algorithm compares the measured fluorescence against the target fluorescence, computes the necessary amount and duration of inducer molecule to provide to the cells to achieve the target fluorescence and moves the syringes accordingly. **(b)** Cellular models. CHO-TETOFF cell line (top) are Chinese Hamster Ovary cells stable expressing the tetracycline-regulated transactivator (tTA) with genomic integration of the tetracycline-repressible promoter (pTRE) upstream of destabilised GFP at both mRNA and protein levels ($Ub^{v76}GFP$) whose expression is repressed in presence of tetracycline. Mouse Embryonic Stem Cells mESC-TETON (middle) stably expressing the reverse tetracycline-regulated transactivator (rtTA) with genomic integration of the tetracycline-inducible pTRE-3G promoter upstream of a destabilised DDmCherry, which is expressed in presence of doxycycline; trimethoprim (TMP) allows protein stabilization. HeLa cell line (bottom) constitutively expressing the TFEB-GFP fusion protein. TFEB-GFP is phosphorylated by mTORC1 and it is cytoplasmic in nutrient-rich medium. mTOR inhibitor Torin-1 induces nuclear accumulation of TFEB-GFP.

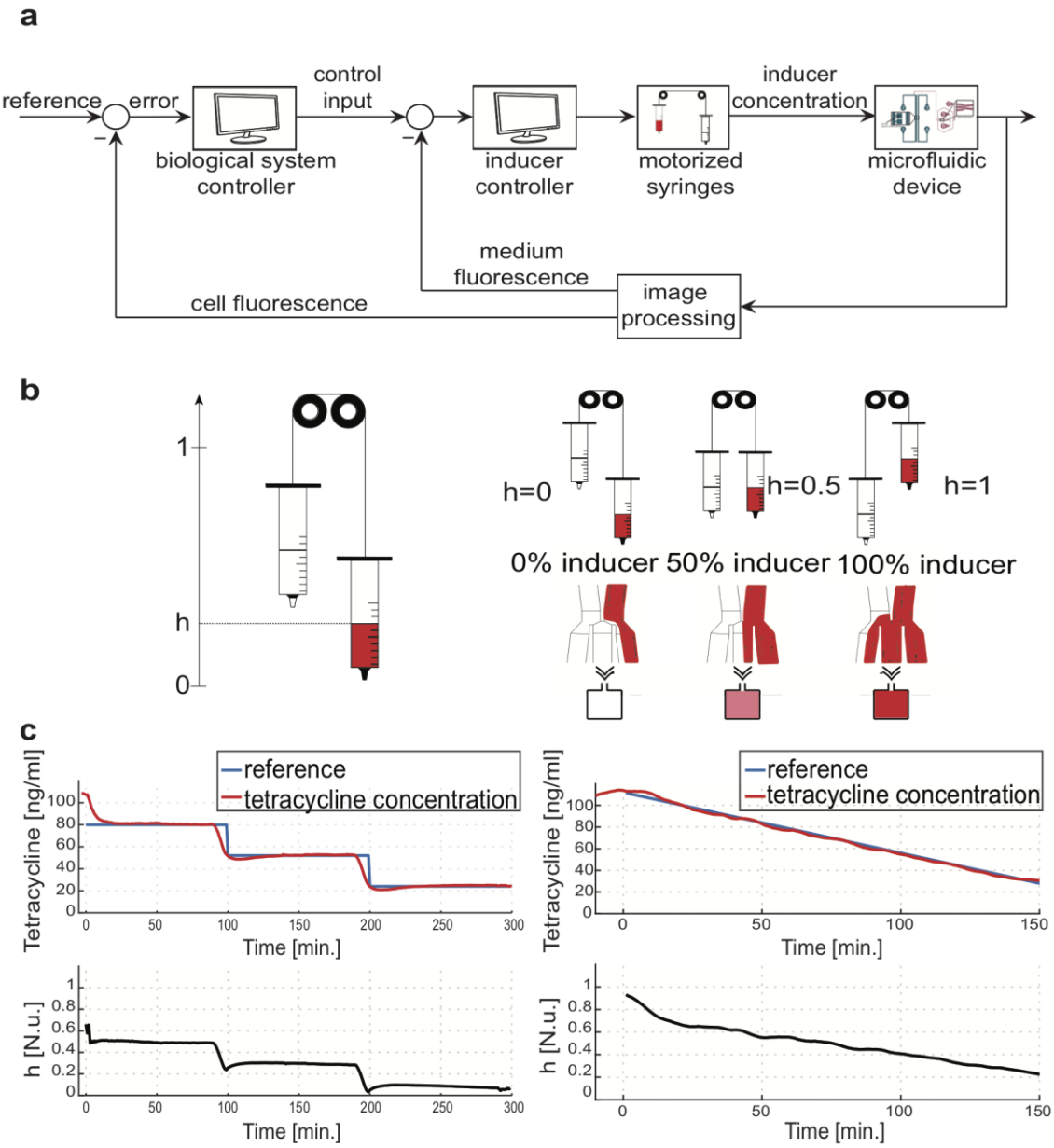

Figure 2. Implementation of closed-loop feedback control. **(a)** Block diagram representation of the control system. The outer negative feedback loop implements the control of the biological system, computing concentration and timing of the inducer molecule (control input) necessary for the measured cell fluorescence to become equal to the target reference value. The inner negative feedback loop implements the inducer molecule control, ensuring that the correct concentration of inducer molecule (control input) is provided to the cells in the microfluidics device. **(b)** Actuation is provided by two motor-controlled syringes constrained to slide on pulleys and filled with either standard growth medium or medium with inducer molecule(s) and fluorescent dye (sulforhodamine). **(c)** *In vitro* tracking control experiments of inducer molecule concentration (red) in a cell chamber of the microfluidic device for two time-varying references (blue). The height of the syringes over time is also shown (black line in the lower panels). The average fluorescence in the cell chamber is imaged at regular intervals (1 minute).

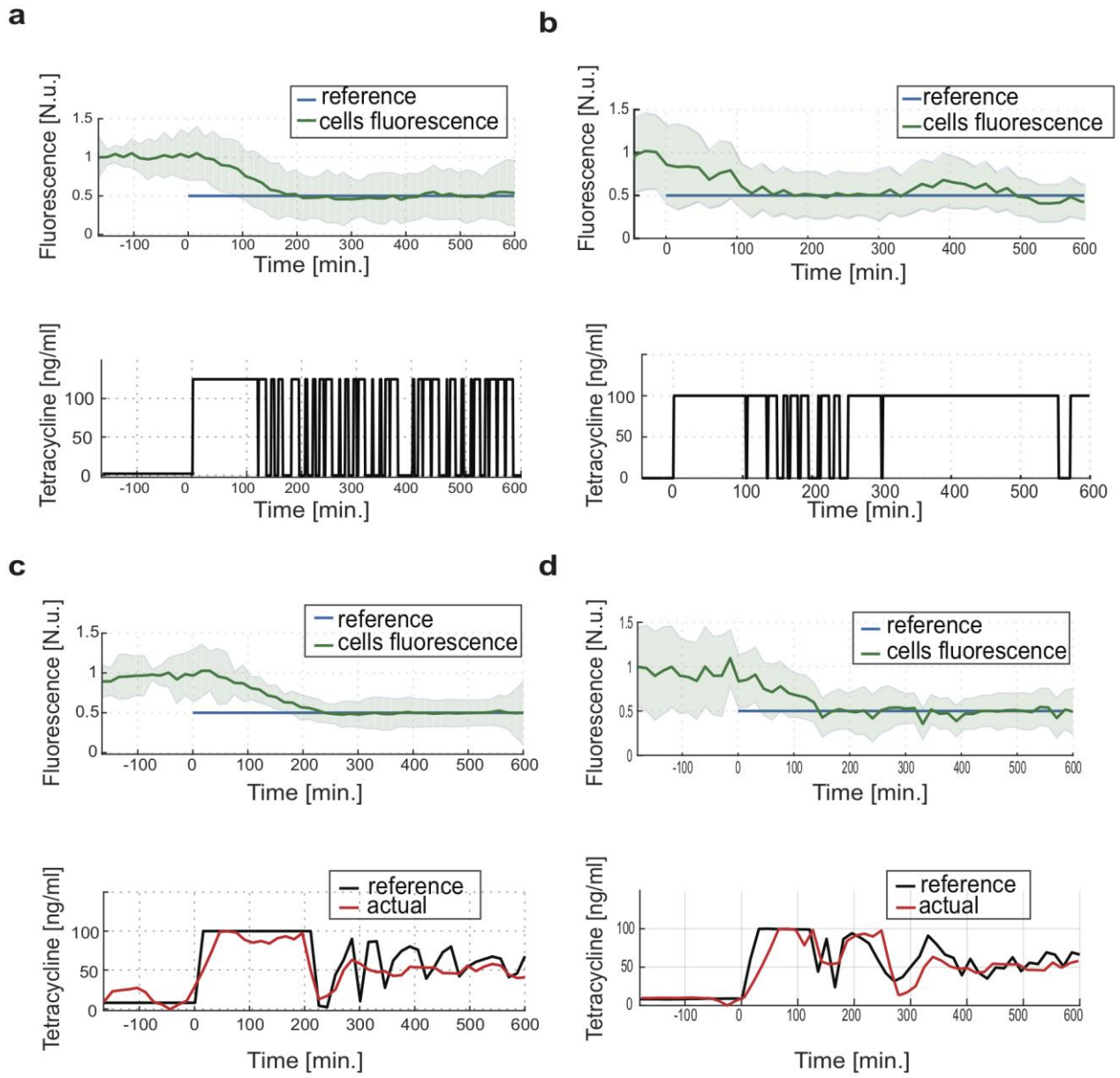

Figure 3. Precise regulation of gene expression from the tetracycline-repressible promoter in CHO-TETOFF cells. Two set-point control experiments are shown using either a fixed concentration of tetracycline **(a,b)** or an arbitrary concentration **(c,d)** as control input (black line in lower panels). The output is the population average fluorescence of $Ub^{V76}GFP$. Control action starts at 0 min. Cells are imaged at sampling time of 15 min. The target value of fluorescence (blue line) is equal to 50% of the cell fluorescence averaged over the population (here normalised to 1) in the absence of tetracycline, during a 180 min calibration phase. The population average cell fluorescence (green line) is shown together with the standard deviation (green shaded area). The desired tetracycline concentration (black line) and the actual tetracycline concentration (red line in c,d) administered to the cells is shown in the lower panels.

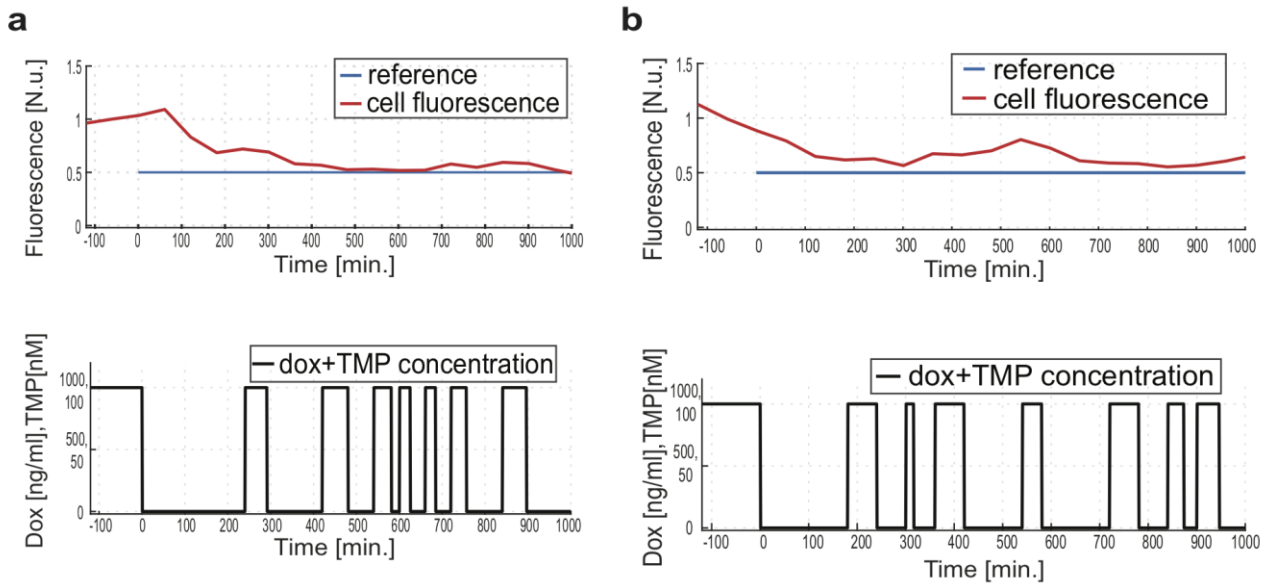

Figure 4. Precise regulation of gene expression from the tet-inducible promoter in mouse Embryonic Stem Cells (mESC-TETON). (a,b) Set-point control experiments using a fixed concentration of Dox+TMP (1000 ng/mL and 100nM respectively) as control input (black line in lower panel). The output is the population average fluorescence of DDmCherry. The control action starts at 0 min. The target fluorescence value (blue line) is 50% of the cell fluorescence averaged over the population (here normalised to 1) in the presence of Dox+TMP during a 120 min calibration phase. Cells are imaged at sampling time of 60 minutes. The population average cell fluorescence (red line in the upper panel) and the control input (Dox+TMP concentration) administered to the cells are shown (black line in the lower panel). Standard deviation is not shown because individual cells could not be resolved by image segmentation algorithm (Supporting Information).

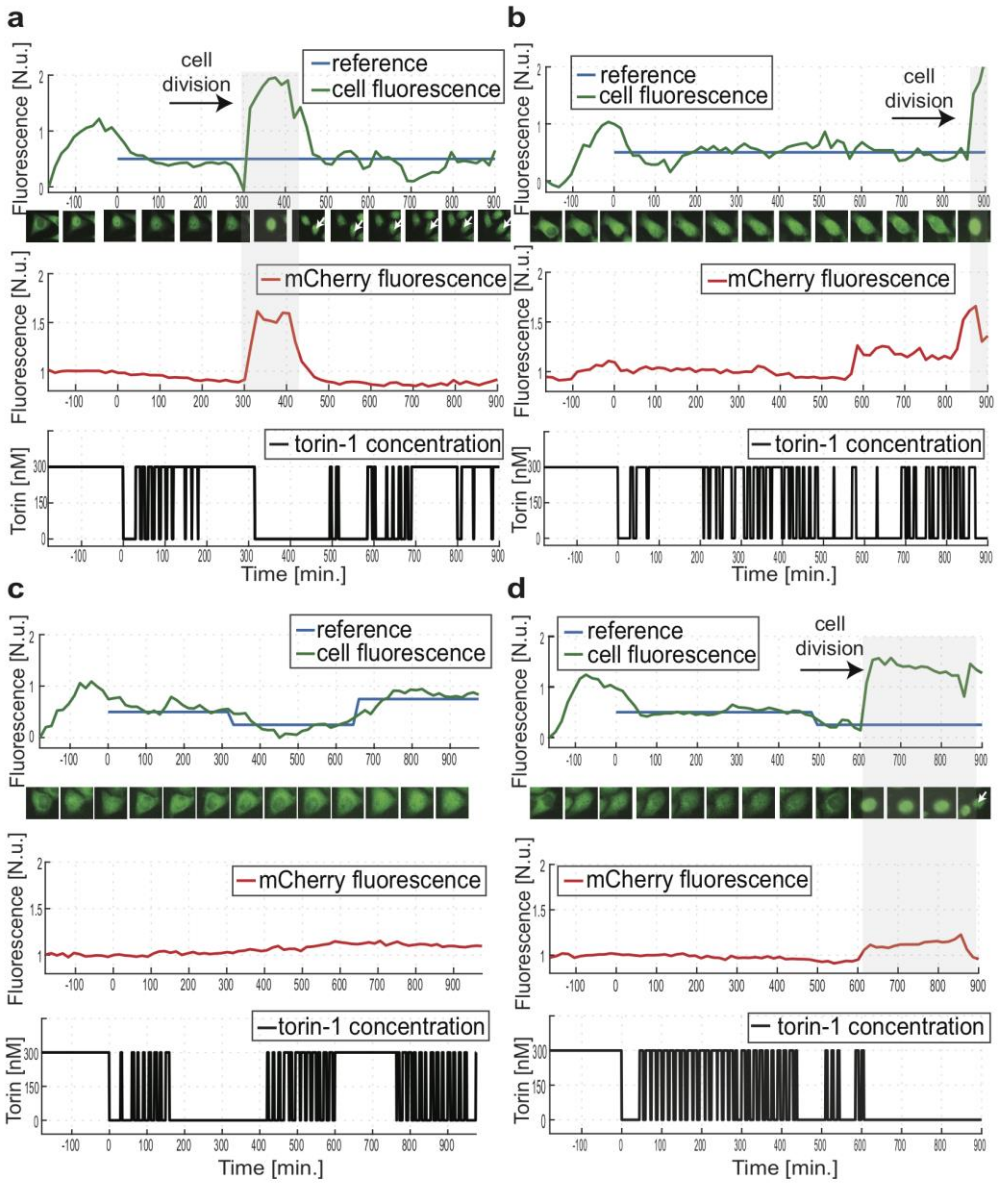

Figure 5. Single-cell control of mTOR signaling in HeLa TFEB-GFP cells. Each panel represents a control experiment in a single-cell. White arrows indicate the controlled cell after cell division has occurred. Two set-point control experiments **(a,b)** and two reference tracking experiments **(c,d)** are shown. During the 180 min calibration phase at the beginning of each experiment, cells are treated with the mTOR inhibitor Torin-1 at the indicated concentrations, which induces maximal TFEB-GFP accumulation in the nucleus (green line). Cell nuclei are tagged with a mCherry fluorescent protein (red line). The TFEB-GFP fluorescence is normalised to the nuclear mCherry fluorescence. Control action starts at 0 min. A fixed concentration of Torin-1 is used as control input (black line). Cell divisions are indicated by grey areas. During cell division both mCherry and TFEB-GFP fluorescence increase due to morphological changes of the nucleus. (**a,b**) Set point control experiments. Target fluorescence value (blue line) is 50% of the TFEB-GFP nuclear fluorescence reached at the end of calibration phase. (**c,d**) Tracking control experiments. The target fluorescence value in **(c)** is time-varying and was chosen equal to 50%, 25% and 75% of the TFEB-GFP nuclear fluorescence reached at the end of calibration phase. The target fluorescence value in **(d)** is also time-varying and was chosen equal to 50% and 25% of the TFEB-GFP nuclear

fluorescence reached at the end of the calibration phase. The longer cell cycle in panel (d) is probably caused by Torin-1 treatment.

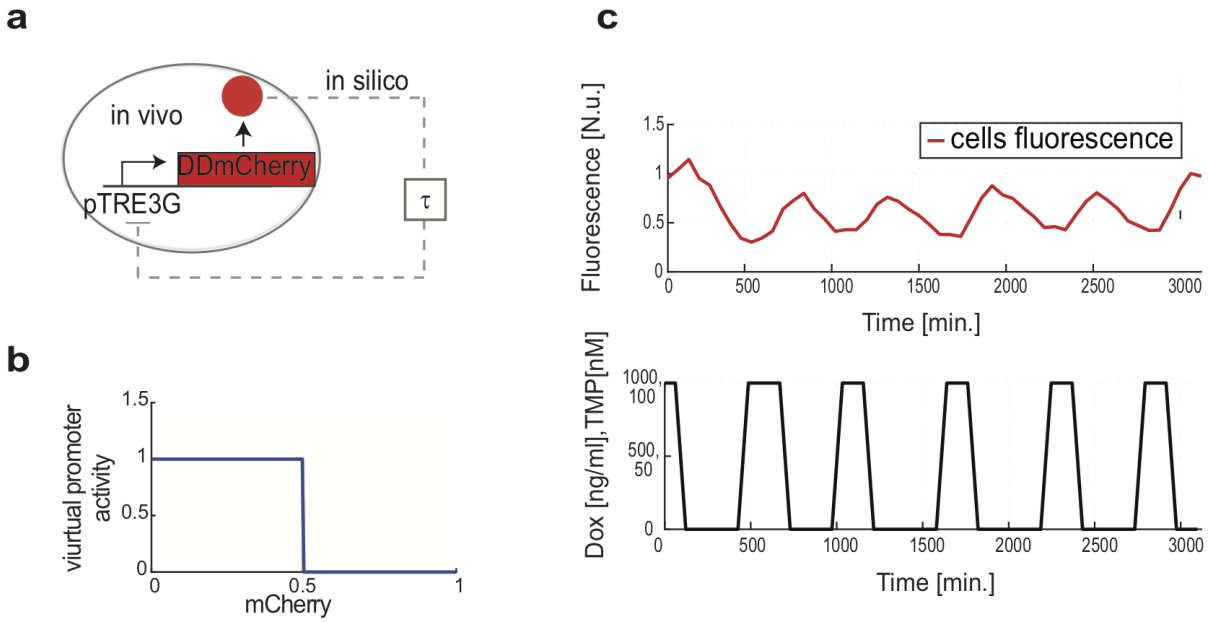

Figure 6. Bio-Hybrid oscillator in mouse embryonic stem cells. (**a**) Schematic representation of the hybrid synthetic circuit implemented in mESCs expressing DDmCherry from the tetracycline-inducible promoter (Figure 1b). DDmCherry represses its own transcription, after a delay τ, thanks to a 'virtual' transcriptional regulation (dashed line) implemented *in silico* via the microfluidics platform. **(b)** Transcriptional regulation is achieved by a 'virtual' DDmCherry responsive promoter driving mCherry expression. If mCherry fluorescence at time t_i is higher than 0.5 normalised units. then a time $t_i + \Delta T$ the promoter is repressed (i.e. standard medium is provided to the cells), where the sampling ΔT=60 min. Vice-versa, the promoter is maximally activated (i.e. Dox+TMP is provided to the cells) if mCherry fluorescence at time t_i is lower than 0.5 normalised units. **(c)** Population average mCherry fluorescence (red line) produced by the Bio-Hybrid oscillator in mESCs. Doxycycline concentration over time is also shown (black line). Standard deviation is not shown because individual mESCs could not be resolved by image segmentation algorithm (Online Methods).